Design and Experimental Testing of a Combustion Nozzle for Use with a Solar Reactor

Jens Heylen[a], Nesrin Ozalp[b,*]

[a]Solar Thermal Technology Laboratory (STTL), KU Leuven, 2860 Sint Katelijna Waver, Belgium
[b]Mechanical and Industrial Engineering Department, University of Minnesota Duluth, 55812 Minnesota, USA
 nozalp@d.umn.edu

It is important to have homogenous temperature distribution inside solar receivers and reactors. This paper presents a methodologic adaptation of a burner nozzle for use with a solar receiver to test and compare the performance of mixing effect of the nozzle with that of used in combustion system. Design steps are described per understanding of the influence of burner nozzle and then creation of a new type of injection port for a solar reactor via adaptive modification. Influence of the nozzle design on the temperature distribution inside a solar reactor is studied per experimental testing of the solar receiver with the new nozzle using a 7 kW high flux solar simulator. Finally, a CFD simulation of the flow pattern inside the solar receiver is given. The results show that it is possible to create different flow patterns inside a solar reactor and enhance the mixing of reactants. The results also show that nozzle provides more homogenous temperature distribution inside the solar reactor. This research demonstrates that implementation of a technique used in a mature field like combustion into solar thermal technology may inspire adaptation of other applications from combustion field to solar thermal field which would accelerate developments in emerging solar thermochemical process technology.

1. Introduction

Solar thermochemistry is an emerging field focusing on the use of concentrated solar radiation for production of fuels and commodities. Solar thermochemical processes take place in solar reactors. Each reactor has its own configuration, size and performance. To maintain production efficiency, it is crucial to have homogenous temperature distribution inside solar reactor. This requires that the heat losses are minimized, and the mass and heat transfer between the reactants promoted. Another important aspect is the concentration of the solar radiation. According to the use of solar radiation as a heat source in the reactor, there are two types of solar reactors: directly and indirectly irradiated reactors. In indirectly heated solar reactor concept, solar radiation heats the external opaque walls of reactor. Heat transfer by conduction and convection from the walls to the reactants provides high temperature process heat for endothermic reactions. A typical example of an indirectly heated reactor is a catalytic tubular reformer designed and tested by Alonso and Romero (2015). That solar reactor concept consists of a tube in which a gas is forced to flow through a catalyst and the solar radiation is exposed along the external walls of the tube. As for direct solar reactors, incoming concentrated solar power is directly used to heat the reactants where the radiation enters reaction chamber through a transparent window. This type of solar reactors are capable of operating at higher temperatures because the reactants are directly exposed to solar radiation. Solar reactors types can also be defined as entrained, fluidized and stacked. Selection of solar reactor type depends on the desired application. For example, fixed bed reactors are recommended for solar catalytic reactions (Ozalp et al., 2013). On the other hand, fluidized beds could be best for reactions requiring high thermal transfer properties. Homogenous heating at the reaction medium is favoured by the close contact between gas and fluidized particles, and higher temperatures are expected to be achieved. It is possible to make the same product through different thermochemical routes with different reactor concepts. However, homogenous distribution of temperature inside solar reactor is the common target of all solar reactor concepts.

Swirling flows are commonly used in industrial applications especially in combustion burners for enhanced burning rate. A swirling flow creates different turbulence flow patterns and enhanced heat transfer inside a reaction chamber. This paper presents the influence of this effect and demonstrates a new type of injection port for a solar reactor exhibiting similar enhancements achieved in combustion chambers.

2. Adaptive design of the nozzle

The original nozzle design is based upon a concept developed by Vanierschot (2007) for a burner, which was successful per experimental observation at the KU Leuven Mechanical Engineering Department and was available for detailed inspection during the course of this research. The most important feature of the nozzle is its capability to create a swirling flow inside the combustion chamber providing intense mixing of the reactant gases. It was expected that adoption of this technology into solar reactor would yield similar flow pattern and homogenous temperature distribution. Figure 1 shows the schematic of burner nozzle designed by Vanierschot (2007).
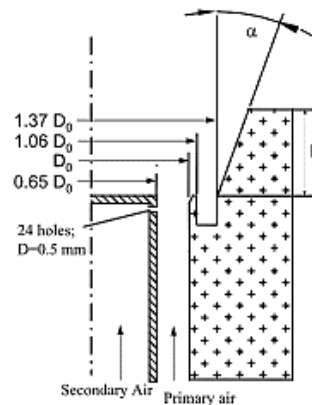
Figure 1: Cross section of the burner nozzle (Vanierschot, 2007)

The nozzle is composed of two parts. There is an inner hollow rod surrounded by an outer part. This design provides two gas streams. The primary gas stream is injected in an annular channel between the inner rod and the outer part. The second stream is injected inside the inner hollow rod. At the end of the rod, there are 24 holes with diameter of 0.5 mm to allow radial injection. This radial injection is the main parameter to control flow pattern inside the reactor. The part outside is a stepped conical nozzle with a slot. Because of the slot, sub-pressure of corner recirculation zone behind the sudden expansion increases. Characteristic dimension of the nozzle is D_o, which is the outer diameter of the annular channel, and the length L is 11.9 mm and $\alpha = 20°$.
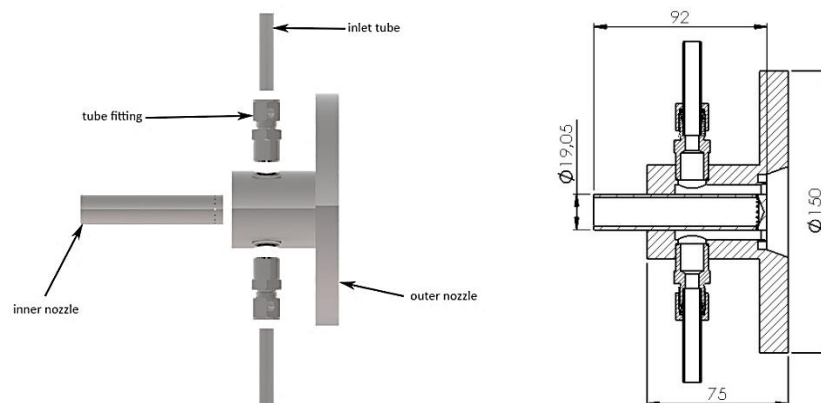
Figure 2: Exploded view of the nozzle designed for solar reactor (left), cross section of the nozzle (right)

To make sure that the nozzle is compatible with the solar reactor, a few adjustments had to be made. To begin with, a flange was attached to the outer nozzle. Then a new method of centralizing the inner rod and the outer part had to be found. To centralize the inner rod with the outer nozzle, the back of the outer part was made

completely closed except for a hole where the inner rod could fit through. To provide the annular channel for air, two injections were symmetrical placed on the sides. The last change on the outer nozzle was the dimensions. To scale the nozzle, the dimension D_o was changed from 27 mm to 29.3 mm. Consequently, all the dimensions depending on D_o were changed as well. Manufacturing limitations required some changes on the inner rod as well. For example, it was too complex to drill 24 holes with a diameter of 0.5 mm on the rod. Therefore, the number of the holes were reduced and the diameters were made bigger. The new inner rod became 16 holes with diameter of 1 mm equally spaced at 3 mm from the end of the rod. An exploded view of the nozzle designed for solar reactor is shown in Figure 2. To hold the inner rod in its place, the inner rod needed to be welded to the outer nozzle. These changes were made in a way so that the flow field is not disturbed.

3. Numerical study of the flow field and temperature distribution inside solar reactor

In order to understand the effect of the nozzle design on the flow field inside the solar reactor, CFD simulations were done. The first objective of the simulations is to see whether the design changes and the scaling of the original nozzle design disturb the flow pattern. After simulating the gas flow inside the reactor, radiative heat transfer is taken into account. Simulation results are compared with experiments for validation. All simulations were done using Ansys Fluent 16.1. For CFD simulations, finite volume method was used where the flow field is divided to finite number of small flow fields. For each element, three conservation equations (mass, momentum and energy) are numerical solved. A complete 3D simulation was made because the new nozzle design is not completely axisymmetric. Conservation of mass:

$$\frac{\partial \varphi}{\partial t} + \nabla * (\varphi u) = 0 \tag{1}$$

Conservation of momentum:

$$\frac{\partial(\rho v)}{\partial t} + \nabla(\varphi v \otimes v) = -\nabla p + \nabla \tau + \varphi \tag{2}$$

Conservation of energy:

$$\varphi \frac{dh}{dt} = \frac{dp}{dt} + \nabla(k\nabla T) + \Phi \tag{3}$$

Since the expected flow field is swirling and has recirculation zones, the realizable k-ε model was used. The model has a good performance for flows involving: rotation, strong pressure gradients and recirculation (Ozalp and Devanuri, 2010). The turbulence kinetic energy, k-equation:

$$\frac{\partial}{\partial t}(\varphi k) + \frac{\partial y}{\partial x_j}(\varphi k u_j) = \frac{\partial}{\partial x_j}\left[\left(\mu + \frac{\mu_t}{\sigma_k}\right)\frac{\partial k}{\partial x_j}\right] + G_k + G_b - \varphi\varepsilon - Y_M + S_k \tag{4}$$

The rate of dissipation, ε-equation:

$$\frac{\partial}{\partial t}(\varphi\varepsilon) + \frac{\partial}{\partial x_j}(\varphi\varepsilon u_j) = \frac{\partial}{\partial x_j}\left[\left(\mu + \frac{\mu_t}{\sigma_\varepsilon}\right)\frac{\partial\varepsilon}{\partial x_j}\right] + \varphi C_1 S\varepsilon - \varphi C_2\frac{\varepsilon^2}{k+\sqrt{v\varepsilon}} + C_{1\varepsilon}\frac{\varepsilon}{k}C_{3\varepsilon}G_b + S_\varepsilon \tag{5}$$

where:

$$C_1 = \max\left[0.43, \frac{\eta}{\eta+5}\right], \quad \eta = S\frac{k}{\varepsilon}, \text{ and } S = \sqrt{2S_{ij}S_{ij}}$$

In order to understand the effect of swirling flow on temperature distribution inside the reactor, radiative heat transfer simulations were done per following governing equation:

$$\frac{\partial}{\partial t}(\rho E) + \nabla * (\vec{v}(\rho E + p)) = \nabla * \left(K_{eff}\nabla T - \sum_j h_j \vec{J_j} + (\overline{\overline{\tau_{eff}}} * \vec{v})\right) + S_h \tag{6}$$

Ansys Fluent features several radiation models, however, the Discrete Ordinates (DO) radiation model is the only model that allows radiation through semi-transparent walls. It is possible to model gray radiation as well as non-gray radiation by using a gray-band model. The use of the non-gray radiation model is necessary for materials that have absorption coefficients that vary stepwise across spectral bands. Behavior of gases which absorb and emit energy at different wavenumbers is not included in the non-gray radiation. The field of modeling non-gray gas radiation is still evolving. By using the Discrete Ordinates model, it is also possible to include scattering, anisotropy and particulate effects in the simulations. The Discrete Ordinates model considers radiation transfer given in Eq(7) as a field equation in the $\vec{s}$ direction.

$$\nabla * (I(\vec{r}, \vec{s})\vec{s}) + (\alpha + \sigma_s)I(\vec{r}, \vec{s}) = an^2\frac{\sigma T^4}{\pi} + \frac{\sigma_s}{4\pi}\int_0^{4\pi} I(\vec{r}, \vec{s}') \phi(\vec{s} * \vec{s}')d\Omega' \tag{7}$$

The discrete ordinates model solves this equation for each discrete solid angle that is associated with a direction vector $\vec{s}$. The angular space 4π is discretized in $N_\theta \times N_\phi$ solid angles with magnitude ω_i for each octant. The control angles θ and φ are the polar and the azimuthal angle respectively. For 3D simulations, 8 octants are solved which makes a total of $8N_\theta N_\phi$ solved directions. The finer the discretization, the more precise the simulation is. A disadvantage of the fine control angles is the increase in computing time because the transport equation is solved for each direction. The boundary conditions of finite volume analyses are used to calculate the discrete values for each variable in the equations. They should define how radiation and flow enters and leaves the computational domain of the reactor. Heat transfer in solar reactor is approximated by two different types of boundary conditions: opaque and semi-transparent walls. The reactor walls are made of stainless steel so they are considered as opaque. The reactor walls are external to the domain because they only have a fluid zone on one side. Although radiation does not transmit through an opaque wall, there are still energy losses at the reactor walls due to external convection and radiation. Conduction through the reactor walls can be simulated by using shell conduction. The incident concentrated solar radiation enters the reactor through a quartz window, which has to be modeled as a semi-transparent boundary condition. The incident radiation flux enters the fluid cell zone through a semi-transparent wall. The transmitted radiation is refracted and dispersed specularly and diffusely. The boundary conditions which control the pheromones are the refractive index and the diffuse fraction. When the refractive index is not equal to 1, a part of the incident radiant is reflected. The incident radiation magnitude is modeled as radiative heat flux (W/m²). The solid angle over which the radiation is distributed is specified as the beam width. Simulations were done for two different geometries. First, reactor without the nozzle, and next, the reactor with nozzle. Once the reactor flow field was defined, it was divided into a finite number of small flow fields. Meshing of the flow field geometry was done via workbench as shown in Figure 3 for both geometries.
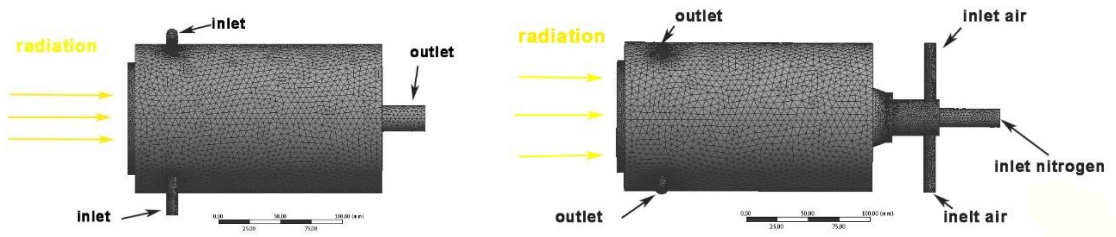
Figure 3: Mesh of the reactor with no nozzle (left), and mesh of the reactor with nozzle (right)

Flow rate of the secondary gas stream is the manipulating parameter to create a certain flow pattern with the nozzle. During the simulations, flow rate of the secondary gas flow needs to be increased to obtain different flow patterns. To obtain that, a transient analysis was done and a velocity profile was used at the secondary inlet. Based on the simulations, velocity of the primary gas flow was set at 1.3 m/s. During tests, the inlet velocity of the secondary gas flow should be small compared to the inlet velocity of the primary gas flow. Air is used as inlet gas for the primary inlet. Nitrogen is used for the secondary inlet.

4. Numerical results

A comparison was made between experimentally obtained flow field per Particle Image Velocimetry (PIV) results of Vanierschot (2007) and the CFD simulated flow field after 10 s of duration. As seen in Figure 4, flow field per CFD looks similar to the experimentally obtained flow field which indicates that this flow pattern could be created by the nozzle inside a solar reactor like it does in burner.
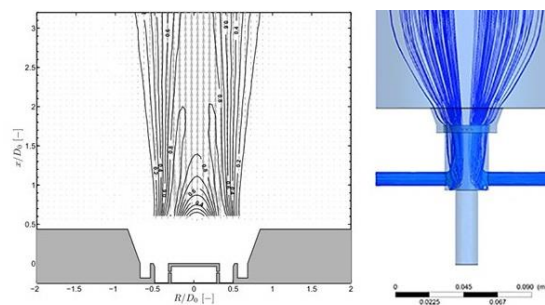
Figure 4: Experimental flow field by Vanierschot (2007) (left), and CFD simulation results (right). At t = 10 s

After 30 seconds, nitrogen velocity reaches to 0.2 m/s. As seen in Figure 5, CFD simulated flow looks similar to experimentally obtained flow which reconfirms that flow pattern similar to the burner can be obtained inside the solar reactor by using the nozzle.
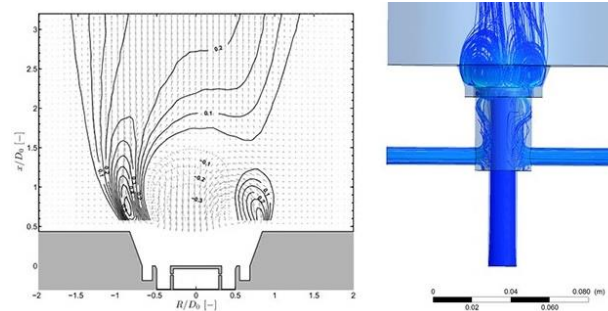
Figure 5: Experimental flow field by Vanierschot (2007) (left), and CFD simulation results (right). At t = 30 s

Results of the heat transfer simulations are shown in Figure 6 for reactor setup with no nozzle, and reactor with nozzle. Both simulations were done with the same boundary conditions to see the impact of the nozzle.
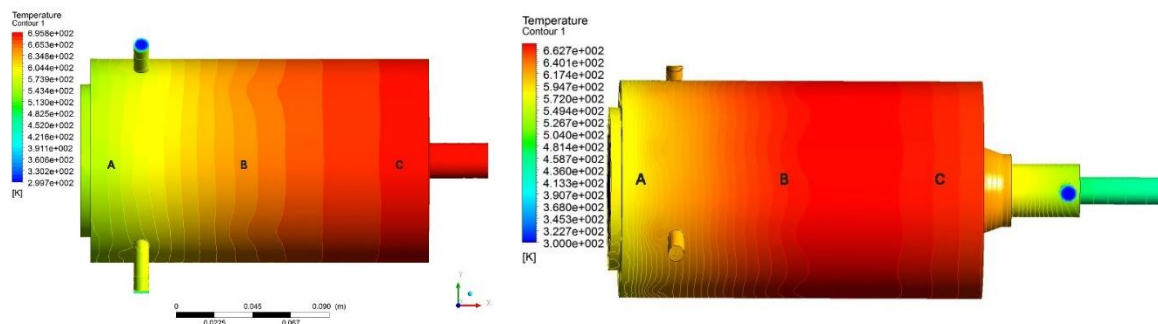
Figure 6: Radiative heat transfer simulations for old reactor setup with no nozzle

By visually comparing both simulation results, it is clear that the nozzle has an impact on the temperature distribution inside the solar reactor. Point marks A, B, and C are used to make comparison with reactor temperatures experimentally measured by using 7 kW high flux solar simulator.

5. Experimental results

Experiments were done using the setup seen in Figure 7. A 7 kW high flux solar simulator was used as the high temperature process heat. The reactor was placed at the focal point of the simulator and the temperature was measured at points A, B and C. Experiments were repeated for reactor with no nozzle and reactor with nozzle.
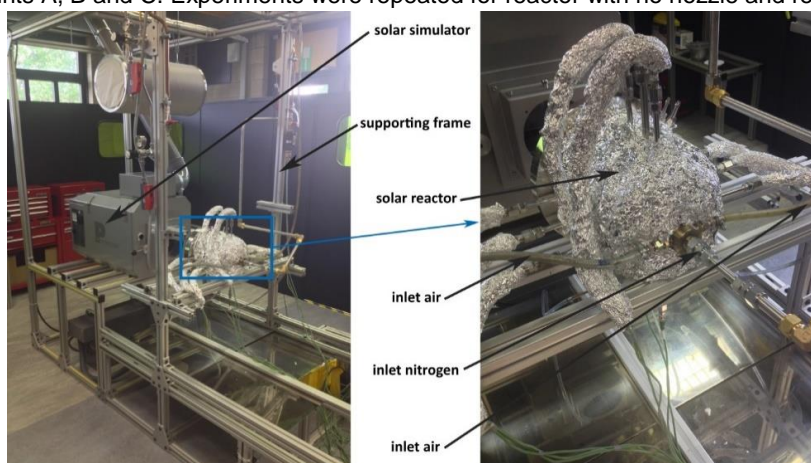
Figure 7: Photo of the experimental setup and the reactor

First experiment was done using reactor without nozzle. The input current was be set at 155 A which represents solar radiation intensity at noon whereas input current of 115 A and 135 A represent solar radiation intensities in the morning and afternoon, respectively (Menon et al., 2013). The second experiment was done with the flow rates obtained from the simulations. Since the nozzle needs two different inlet flow rates, an additional air flow was provided on top of nitrogen flow where air velocity was 1.3 m/s, and nitrogen velocity was 0.3 m/s. The data of this experiment was used as reference. The third experiment was done with a total flowrate of 10 L/min. However, the air/nitrogen ratio was kept the same as in experiment #2. This experiment was done with a total flowrate of 10 L/min. Air and nitrogen flowrates were the same as in experiment #3. The changed parameter for this experiment is the input current which was set at 115 A. That experiment was done with a total flowrate of 10 L/min. The air and nitrogen flowrates were the same as in experiment #3. The changed parameter for this experiment is the input current which was set at 135 A. Table 1 gives an overview of the experimental data measured. Temperature differences can only be compared between the first three experiments due to the power level. It is seen that the nozzle has favourable impact on the temperature distribution inside the reactor.

Table 1: Summary of the experiment results

Result type	Setup	Temperature at A [°C]	Temperature at B [°C]	Temperature at C [°C]
Simulation	Without nozzle	155	355	316
Experiment 1	Without nozzle	155	322	289
Simulation	With nozzle	155	342	307
Experiment 2	With nozzle	115	228	203

In general, we can conclude that the temperatures in point C are in the same range, however, there is a significant difference between the temperature in point A and B. It should be noted that the simulated model is based on a flow field surrounded by shell conduction layers which represents the opaque reactor walls. It seems that the amount of heat transferred by conduction through the boundary shells is not comparable by the amount that is transferred by the stainless-steel walls of the solar reactor. To obtain more accurate simulation results, the reactor can be modelled with less simplifications. For example, the reactor can be fully 3D modelled instead of the shell layers, however, this would increase the computation time drastically.

6. Conclusions

A nozzle type inlet design inspired from a burner was tested for a solar reactor. It was an iterative design process based on CFD simulations. Once the nozzle was fully designed, numerical radiative heat transfer simulations estimated the effect of the nozzle design in comparison to the same reactor without nozzle. Due to its geometry, the nozzle creates different flow patterns inside the reactor. The goal was to make the temperature distribution inside the reactor more homogenous. At the end, the nozzle was tested by experiments and the CFD simulations were compared with experiments. Although the nozzle design was successful and made the temperature distribution inside the reactor more homogenous, the difference between the temperature in front of the reactor and the temperature at the back of the reactor was higher than targeted. However, it was concluded that it is possible and helpful to use nozzle or similar apparatus from traditional combustion systems as a starting point or preliminary work in solar thermochemical systems.

Acknowledgment

References

Alonso E., Romero M., 2015, Review of Experimental investigation on Directly Irradiated Particles Solar Reactors, Renewable and Sustainable Energy Reviews, 41, 53–67.

Menon A., Asadullah F., Ozalp N., 2013, A New Solar Reactor Aperture Mechanism Coupled with Heat Exchanger, Chemical Engineering Transactions, 35, 751–756.

Ozalp N., Ibrik K., Al-Meer M., 2013, Kinetics and Heat Transfer Analysis of Carbon Catalysed Solar Cracking, Energy, 55, 74–81.

Ozalp N., Devanuri J., 2010, CFD Analysis of Multi-Phase Turbulent Flow in a Solar Reactor for Emission-free Generation of Hydrogen, Chemical Engineering Transactions, 21, 1081–1086.

Vanierschot M., 2007, Fluid Mechanics and Control of Annular Jets with and without Swirl, PhD thesis, Department of Mechanical Engineering, KU Leuven, The Netherlands.